

# Study of low-lying electronic states of ozone by multireference Møller–Plesset perturbation method

T. Tsuneda, H. Nakano, and K. Hirao

Department of Applied Chemistry, Graduate School of Engineering, The University of Tokyo, Tokyo, Japan 113

(Received 12 June 1995; accepted 18 July 1995)

The geometry and relative energy of the seven low-lying electronic states of ozone and the ground state of ozonide anion have been determined in  $C_{2v}$  symmetry by the complete active space self-consistent field (CASSCF) and the multireference Møller–Plesset perturbation (MRMP) methods. The results are compared with the photodetachment spectra of  $O_3^-$  observed recently by Arnold *et al.* The theoretical electron affinity of ozone is 1.965 eV, which is 0.14 eV below the experimental result of 2.103 eV. The calculated adiabatic excitation energies (assignment of Arnold *et al.* in parentheses) of ozone are  $^3A_2$  0.90 eV (1.18 eV),  $^3B_2$ , 1.19 eV (1.30 eV),  $^3B_1$ , 1.18 eV (1.45 eV),  $^1A_2$ , 1.15 eV (~1.6 eV),  $^1B_1$ , 1.65 eV (2.05 eV), and  $^1B_2$ , 3.77 eV (3.41 eV), respectively. Overall the present theory supports the assignment of Arnold *et al.* However, the simple considerations of geometry and energy are insufficient to determine a specific assignment of the  $^3B_2$  and  $^3B_1$  states. The dissociation energy of the ground state of ozone is computed to be 0.834 eV at the present level of theory. The present theory also predicts that none of the excited states lies below the ground state dissociation limit of  $O_3$ . © 1995 American Institute of Physics.

## I. INTRODUCTION

In order to understand the underlying chemistry and physics of ozone depletion, a wide range of laboratory experimental and theoretical studies have been directed towards the characterization of the  $O_3$  dissociation dynamics and electronic structure. Our understanding of this fundamental molecule has improved greatly but still there are many puzzling phenomena.

The diradical character of ozone leads to the existence of several low-lying excited states. The fact that ozone absorbs weakly in the visible and near-infrared was first noted by Chappuis<sup>1</sup> and Wulf,<sup>2</sup> respectively. The symmetry allowed transition from the ground state is only the  $^1B_1 \leftarrow X^1A_1$  transition and  $^1A_2 \leftarrow X^1A_1$  transition is vibronically allowed via the  $\nu_3$  antisymmetric stretch. The remaining low-lying electronic states are triplet states. Two absorption bands in this region implies some form of coupling to enable absorption to at least one dark electronic state. Chappuis and Wulf bands were assigned with the aid of early *ab initio* results to the  $^1B_1 \leftarrow X^1A_1$  and  $^1A_2 \leftarrow X^1A_1$  transitions, respectively. Recently Anderson *et al.*<sup>3,4</sup> re-examined the Wulf and Chappuis bands and measured the isotopic shifts of the absorption spectra of  $^{16}O_3$  and  $^{18}O_3$ . They concluded that the weaker Wulf band is more likely due to the  $^1A_2$  state and that the stronger Chappuis band is due to the absorption of two electronic states; namely the  $^1B_1$  state and a still unassigned state. On the other hand, Vaida *et al.*<sup>6</sup> concluded that the Chappuis band is due mainly to the  $^1A_2$  state, based on their measurements of condensed phase absorption of ozone. Theoretical studies by Braunstein *et al.*<sup>7–9</sup> and Banichevich *et al.*<sup>10–12</sup> showed that the Chappuis band results from the significant interaction between the  $^1B_1$  and  $^1A_2$  states. This implies that low-lying Wulf band is due to transitions to one or more triplet states. Anderson *et al.*<sup>5</sup> reassigned the spectrum and concluded the weaker Wulf band is due to the  $^3A_2$

by the analysis of the rotational structure of the spectrum.

Several techniques other than photoabsorption have been used to study  $O_3$  in the visible and near-infrared regions.<sup>13–17</sup> Some of them suggested the existence of energy levels which are bound with respect to the dissociation.<sup>18–20</sup> There are three electronic states in addition to the  $^1A_1$  ground state which correlate with  $O(^3P) + O_2(^3\Sigma_g^-)$ . These are the  $^3A_2$ ,  $^3B_2$ , and  $^1A_2$  states and these lie near the dissociation threshold of the ground state ( $D_0=1.05$  eV;  $D_e=1.13$  eV). However, no complete state assignment exists and some uncertainty remains concerning whether there are bound electronic excited states. The  $2^1A_1$  and  $^3A_1$  states also correlate with the ground state dissociation limit but these are predicted to lie well above the dissociation limit.

Very recently Arnold *et al.*<sup>21</sup> provided a more complete picture of the  $O_3$  electronic and vibrational structure by the analysis of the anion photoelectron spectroscopy of  $O_3^-$ . They observed transitions to five lowest excited states of  $O_3$  below 3 eV in energy;  $^3A_2$ ,  $^3B_2$ ,  $^3B_1$ ,  $^1A_2$ , and  $^1B_1$  states. They assigned the transitions tentatively with the help of the previous calculations. Of importance is the fact that they did not observe any evidence of electronic states lying below the ground state dissociation asymptote. The large amount of vibrational structure above the dissociation limits of the excited states suggests that interesting dissociation dynamics occurs on these surfaces.

The  $O_3^-$  ion is believed to be an important intermediate in the  $D$  region of the earth's ionosphere. The  $O_3^-$  has not been observed by high resolution spectroscopic techniques although the frequencies of the  $\nu_1$  symmetric stretching and  $\nu_2$  bending bands have been fairly well determined in the gas-phase by photodissociation,<sup>22</sup> photodetachment,<sup>23</sup> and photoelectron<sup>24</sup> spectroscopy. The laser photoelectron work of Novick *et al.*<sup>24</sup> and the photodetachment spectrum of Wang *et al.*<sup>23</sup> also provided estimates of the equilibrium structure of  $O_3^-$  through Franck–Condon analysis. Much of

the experimental work of this radical has been carried out in the rare gas matrices by Raman or infrared spectroscopy usually in the presence of cerium or sodium counterions.

In an attempt to provide a more reliable characterization of the excited states of  $O_3$ , we have studied six lowest excited states of ozone using multireference Møller–Plesset perturbation method (MRMP), which has been successful in recent years in predicting details of molecular electronic spectra.<sup>25–29</sup> We explored a range of  $C_{2v}$  geometries around the minima of these states of ozone as well as the ground state of ozonide anion. In this paper we will report the properties of low-lying excited states of  $O_3$  and present an interpretation of the photodetachment spectra of  $O_3^-$ .

The focus is the explanation for the experimentally determined adiabatic excitation energies and observed vibrational progressions in the photodetachment spectra of  $O_3^-$ .

Section II summarizes the computational details and calculated results and discussions will be given in Sec. III. Conclusions will be summarized in the final section.

## II. METHOD OF CALCULATIONS

The calculation was carried out for the ground and low-lying singlet and triplet excited states of ozone and the ground state of ozonide anion. All calculations were performed with a triple-zeta plus polarization quality basis of Dunning's cc-pVTZ (Ref. 30) augmented with the diffuse functions ( $1s1p1d$ ). The diffuse functions are indispensable particularly to describe  $O_3^-$  and the ionic  ${}^1B_1$  excited state of  $O_3$  (all other states treated here are covalent states). As has been pointed out previously, the ground state of ozone can be viewed as two distinct spatial configurations (with the exception of the  ${}^3B_2$  state where a single configuration suffices). Thus, the active space of the CASSCF should be chosen large enough such that all near degeneracy effects are included and the accurate assessment of the relative energies will require the explicit inclusion of additional dynamical correlation effects. All valence 18 (19 for  $O_3^-$ ) electrons are treated as active electrons and distributed among all valence 12 orbitals. The complete state-specific CASSCF (Refs. 31–33) calculation is carried out for each individual state with proper spin and symmetry to obtain an optimal geometry. The range of coordinates in  $C_{2v}$  symmetry are 1.1–1.7 Å in steps of 0.05 Å for the bond length and 75.0° to 135.0° in steps of 5° for the bond angle. By analytically fitting these two-dimensional grid points, we obtained the entire potential energy surfaces and calculated properties for the ground and excited states. The higher level of MRMP was only used to calculate excitation energy at minimum point of each individual state. Oxygen  $1s$  orbitals were optimized in the CASSCF calculations but were uncorrelated in the MRMP calculations. Vertical excitation energies were computed at the experimental geometry for the ground state of ozone at the MRMP level. Adiabatic excitation energy for each state was determined by computing the MRMP energy at the calculated geometry for the state and subtracting the energy of the ground state at its calculated geometry. The  $\nu_1$  and  $\nu_2$  vibrational frequencies were calculated with CASSCF and used to estimate the zero-point energy (ZPE) corrections. The  $\nu_3$  vibrational frequencies are not available and its con-

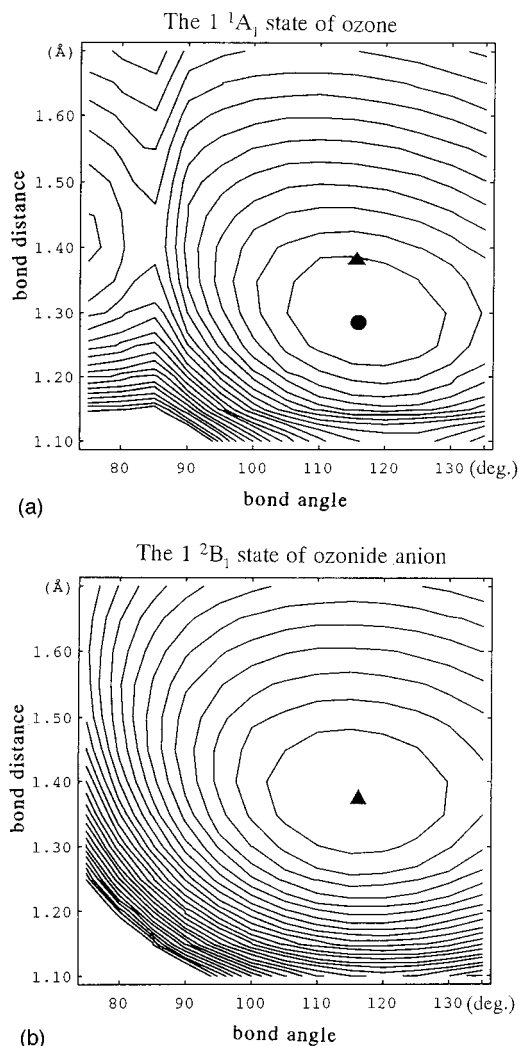


FIG. 1. Electronic energies of the ground states of ozone and ozonide anion as a function of bond angle and bond length for the  $C_{2v}$  geometry. Points are calculated every 5° and 0.05 Å. The dot and triangle show the minimum points of the ground state of ozone and the ozonide anion, respectively. The contours increase monotonically in steps of 0.01 a.u. from the minimum point.

tribution to the ZPE is not considered here. The transition moments were also calculated at the level of CASSCF approximation.

## III. CALCULATED RESULTS AND DISCUSSIONS

In Fig. 1 we show contour diagrams summarizing results from CASSCF calculations of the ground state of ozone and its anion in  $C_{2v}$  symmetry. The contour plots of the excited states of ozone are summarized in Fig. 2. The minimum point and the Franck–Condon projection from the ozonide anion are also shown in each contour map. Conical intersections between  ${}^3A_2$  and  ${}^3B_1$  states and between  ${}^1A_2$  and  ${}^1B_1$  states are also drawn in Fig. 2.

The CASSCF configurations for the various states of ozone in terms of  $C_{2v}$  symmetry orbitals are given in Table I. The CASSCF wave function for the ground state of ozone is

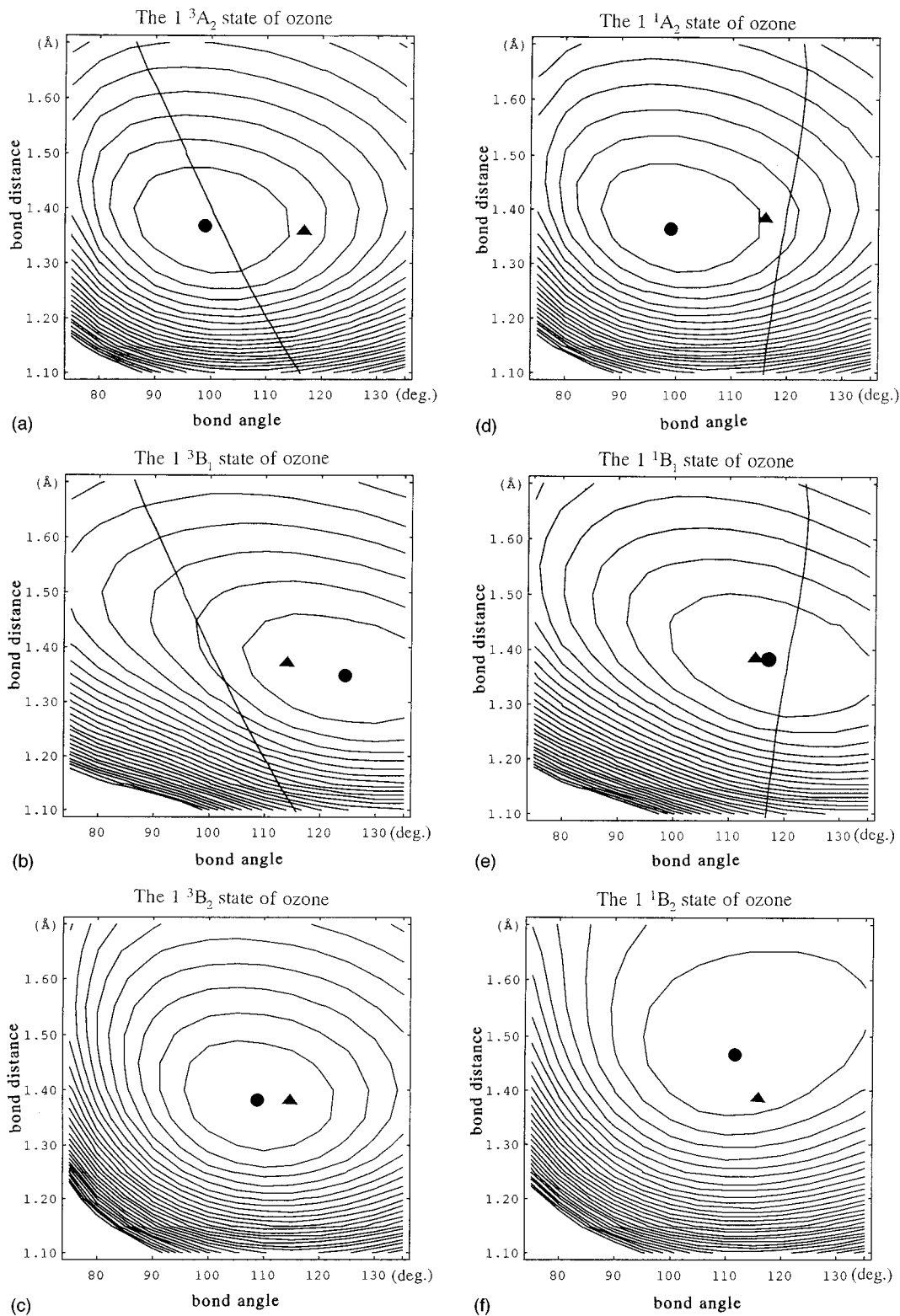


FIG. 2. Electronic energies of the excited states of ozone as a function of bond angle and bond length for the  $C_{2v}$  geometry. Points are calculated every  $5^\circ$  and  $0.05 \text{ \AA}$ . The dot shows the minimum point of each excited state of ozone and the triangle shows the Franck–Condon projection from the ground state of ozonide anion. The contours increase monotonically in steps of  $0.01 \text{ a.u.}$  from the minimum point. The line crossing the contours in  $^3A_2$  and  $^3B_1$  states is the seam where the two states are degenerate. The seam between  $^1A_2$  and  $^1B_1$  states is also drawn.

TABLE I. Types of transitions in ozone and CI coefficients of CASSCF wave function.

State	Coefficients	Configurations <sup>a</sup>							
		6a <sub>1</sub>	4b <sub>2</sub>	1b <sub>1</sub>	1a <sub>2</sub>	2b <sub>1</sub>	7a <sub>1</sub>	5b <sub>2</sub>	
<sup>1</sup> A <sub>1</sub>	0.9045	2	2	2	2	0	0	0	Ψ <sub>A</sub>
	-0.2946	2	2	2	0	2	0	0	Ψ <sub>B</sub>
<sup>3</sup> A <sub>2</sub>	0.8844	2	1	2	2	1	0	0	Ψ <sub>A</sub> (4b <sub>2</sub> →2b <sub>1</sub> )
	-0.3400	1	2	2	1	2	0	0	Ψ <sub>B</sub> (6a <sub>1</sub> →1a <sub>2</sub> )
<sup>3</sup> B <sub>2</sub>	0.9537	2	2	2	1	1	0	0	Ψ <sub>A</sub> (1a <sub>2</sub> →2b <sub>1</sub> ) or Ψ <sub>B</sub> (2b <sub>1</sub> →1a <sub>2</sub> )
<sup>3</sup> B <sub>1</sub>	0.8889	1	2	2	2	1	0	0	Ψ <sub>A</sub> (6a <sub>1</sub> →2b <sub>1</sub> )
	-0.3160	2	1	2	1	2	0	0	Ψ <sub>B</sub> (4b <sub>2</sub> →1a <sub>2</sub> )
<sup>1</sup> A <sub>2</sub>	0.8605	2	1	2	2	1	0	0	Ψ <sub>A</sub> (4b <sub>2</sub> →2b <sub>1</sub> )
	-0.4001	1	2	2	1	2	0	0	Ψ <sub>B</sub> (6a <sub>1</sub> →1a <sub>2</sub> )
<sup>1</sup> B <sub>1</sub>	0.8359	1	2	2	2	1	0	0	Ψ <sub>A</sub> (6a <sub>1</sub> →2b <sub>1</sub> )
	-0.4468	2	1	2	1	2	0	0	Ψ <sub>B</sub> (4b <sub>2</sub> →1a <sub>2</sub> )
<sup>1</sup> B <sub>2</sub>	0.7051	2	2	2	1	1	0	0	Ψ <sub>A</sub> (1a <sub>2</sub> →2b <sub>1</sub> )
	-0.4074	2	2	1	1	2	0	0	Ψ <sub>B</sub> (1b <sub>1</sub> →1a <sub>2</sub> )
	-0.3310	2	1	2	0	2	1	0	Ψ <sub>B</sub> (4b <sub>2</sub> →7a <sub>1</sub> )
	0.2113	1	2	2	2	0	0	1	Ψ <sub>A</sub> (6a <sub>1</sub> →5b <sub>2</sub> )

<sup>a</sup>The 1b<sub>1</sub>, 1a<sub>2</sub>, and 2b<sub>1</sub> are π orbitals, perpendicular to the molecular plane while 6a<sub>1</sub> and 4b<sub>2</sub> are in-plane lone-pair orbitals.

represented by two configurations, the Hartree–Fock configuration and π→π\* double excitation, (1a<sub>2</sub>)<sup>2</sup>→(2b<sub>1</sub>)<sup>2</sup> configuration

$$[\text{core}](3a_1)^2(2b_2)^2(4a_1)^2(5a_1)^2(3b_2)^2(1b_1)^2 \\ (6a_1)^2(4b_2)^2[0.905(1a_2)^2 - 0.295(2b_1)^2] + \dots$$

Other low-lying excited states except the <sup>3</sup>B<sub>1</sub> state also require at least two spatial configurations. The configurations relative to the Hartree–Fock and π→π\* (1a<sub>2</sub>)<sup>2</sup>→(2b<sub>1</sub>)<sup>2</sup> configurations are also listed in the table. These excited states are covalent in nature except the <sup>1</sup>B<sub>2</sub> state and are basically represented by single excitations relative to the ground state configurations. The <sup>1</sup>B<sub>2</sub> state is an ionic state and is a mixture of singly excited configurations but includes a fairly large fraction of the doubly excited configurations. On the other hand, the anion state <sup>2</sup>B<sub>1</sub> can be well described by a single configuration in C<sub>2v</sub> symmetry as

$$[\text{core}](3a_1)^2(2b_2)^2(4a_1)^2(5a_1)^2(3b_2)^2(1b_1)^2(6a_1)^2 \\ (4b_2)^2(1a_2)^2(2b_1)^1.$$

Judging from the characteristics of the CASSCF wave functions, we can expect that the <sup>3</sup>B<sub>1</sub> state is well described even at the level of CASSCF but inclusion of dynamical correlation effects through MRMP will make a significant contribution to the positions of other excited states, particularly to the <sup>1</sup>B<sub>2</sub> state.

### A. The ground states of ozone and ozonide anion

The optimized geometry of the ground state from CASSCF calculations is in good agreement with experiment. The predicted bond length (*r*<sub>e</sub>) of 1.291 Å is slightly (0.02 Å) longer than the best experimental value of 1.2717 Å. The theoretical bond angle (*θ*<sub>e</sub>) of 116.6° differs only by 0.1° from the experimental value of 116.7°. Our results are very close to the previous MRD-CI results.<sup>9</sup> The state-specific CASSCF and MRMP gave -224.573 95 a.u. and -225.095 44 a.u. at this geometry, respectively. The poten-

tial energy surface of the ground state of ozone has the double minima, the open structure (C<sub>2v</sub>) and the equilateral triangle ring structure (D<sub>3h</sub>). The latter state is dominated by the π→π\* doubly excited configuration. We can see immediately from the contour plot of ozone shown in Fig. 1 that contours have the conical intersection of these two states along nearly vertical line where *θ* has a value of about 85.5°.

Optimized anion geometric parameters are *r*<sub>e</sub>=1.376 Å and *θ*<sub>e</sub>=115.5°. The present calculation predicts a longer bond length and a larger bond angle than those in the gas-phase obtained by Franck–Condon analysis of the photodetachment observation by Wang *et al.*<sup>23</sup> (*r*<sub>e</sub>=1.3415±0.03 Å and *θ*<sub>e</sub>=112.6°±2.0°). However, comparison of the ozonide geometry obtained from the previous calculations<sup>34–36</sup> and the present work finds reasonable agreement in many cases, especially for a bond angle. For instance, the best estimated values by Koch *et al.*<sup>35</sup> are *r*<sub>e</sub>=1.35 Å and *θ*<sub>e</sub>=114.5°. Table II summarized the electron affinity and dissociation energy of ozone. The computed electron affinity of ozone is 1.965 eV (ZPE correction is included) at the MRMP level, which

TABLE II. Calculated and experimental dissociation energy and electron affinity of ozone.<sup>a</sup>

Method	<i>D</i> <sub>e</sub> (eV)	EA <sub>a</sub> (eV)
MP4 <sup>b</sup>	1.80	1.69
MRCI <sup>b</sup>	2.04	1.92
CASPT2 <sup>c</sup>	0.82	2.18
CASPT2( <i>g</i> <sub>2</sub> ) <sup>c</sup>	1.08	2.22
MRMP	0.834	1.965
Expt. <sup>d</sup>	1.13	2.103

<sup>a</sup>ZPE corrections are added to the electron affinity.

<sup>b</sup>Reference 25.

<sup>c</sup>Reference 41.

<sup>d</sup>Reference 21.

can be compared to the experimental value of  $2.1028 \pm 0.0025$  eV determined by Novick *et al.*<sup>24</sup> using threshold photodetachment. The MRMP underestimates the electron affinity only by 0.14 eV while CASPT2 overestimates the electron affinity. It is noted that a single reference based method such as MP4 gives a poor description of the electron affinity. The dissociation energy of the ground state,  $D_e$ , is computed to be 0.834 eV at the same level of theory, which is within 0.30 eV of the experiment of 1.13 eV.

The photoelectron spectrum measured by Arnold *et al.*<sup>21</sup> with a photodetachment energy of 2.977 eV shows the vibrational progressions, which provides information about the changes in equilibrium geometry between  $O_3^-$  and  $O_3$ . The long symmetric stretch progression indicating that there is a significant difference between the bond lengths of the anion and neutral is consistent with our results (see Fig. 1). The spectrum also shows the shorter progression in the bending modes, implying that the bond angle also differ but not as substantially. It is expected that the removal of electron from a  $2b_1$  antibonding  $\pi$  orbital should lead to an increase of a bond angle but the present calculation shows that the change of a bond angle is rather insensitive to an electron detachment.

## B. Vertical excitation energies

Vertical excitation energies and oscillator strengths are summarized in Table III. We carried out MRMP calculations based on the state-specific CASSCF wave function at the experimental geometry ( $r_e=1.2717$  Å,  $\theta_e=116.7^\circ$ ). Results with the state-averaged CASSCF plus MRMP are also listed in parentheses in the table. Oscillator strengths were calculated by using transition moments computed at the CASSCF level and the MRMP transition energies. The results have been compared with data from the previous calculations available; the polarization configuration interaction (POL-CI),<sup>37,38</sup> the multiconfigurational SCF plus configuration interaction (MCSCF-CI),<sup>12</sup> the multireference based doubly excited configuration interaction method (MRD-CI),<sup>9</sup> and the Fock space multireference coupled-cluster (FSM-RCC) method.<sup>39</sup> In all cases a double-zeta plus polarization quality basis set has been used. The comparison with the multiconfiguration linear response (MCLR) (Ref. 40) with a larger basis has also been made. In preparing the paper, the multiconfigurational second-order perturbation [CASPT2 and CASPT2( $g_2$ )] results have been reported by Borowski *et al.*<sup>41</sup> and cited in the table.

The present calculation indicates the five lowest states lie at less than 2 eV above the ground states. MRMP with state-specific CASSCF gives larger excitation energies compared to MRMP with state-averaged CASSCF although the difference is minor. Most studies found the three triplet states  $^3B_1$ ,  $^3B_2$ , and  $^3A_2$  to be lowest in energy. Our MRMP vertical excitation energies,  $T_v$ , are 1.51 eV (1.47 eV) for  $^3B_1$ , 1.65 eV (1.57 eV) for  $^3A_2$  and 1.71 eV (1.56 eV) for  $^3B_2$ , respectively. However, the ordering is not necessarily the same in other theoretical studies. This is understandable because of the small energetic separation between the three states. The MRMP predicts that three triplet states are very close in energy and the spacing is less than 0.2 eV. There are no experi-

mental values for the  $^3B_1$  and  $^3A_2$  states but the  $^3B_2$  excitation energy is estimated to be  $\sim 1.7$  eV. Our computed  $^3B_2$  excitation energy of 1.71 eV is close to the experimental value.

The states following three triplet states are the singlet states  $^1A_2$ , 1.88 eV (1.78 eV) and  $^1B_1$ , 1.97 eV (1.87 eV). The present excitation energies for  $^1A_2$ , and  $^1B_1$  states are in reasonable agreement with the experimental values;  $^1A_2$ , 1.6 eV, and  $^1B_1$ , 2.1 eV. The intensity of  $^1B_1$  state is very low as expected. We can see in Table III that the oscillator strength is also reproduced well. The  $^1B_2$  state is computed to lie 4.81 eV (4.62 eV) above the ground state. It is clearly related to the most intense feature of the  $O_3$  spectra (Hartley band). Peaks around 4.86 eV were reported as the vertical excitation energy, which is in good agreement with the calculated value of 4.82 eV. Previous theoretical calculations have obtained considerably larger transition energies. The  $^1B_2$  state is an ionic excited state. As shown in Table I, the wave function is dominated by the transition of  $\pi \rightarrow \pi^*$  but includes a large fraction of other singly and doubly excited configurations. Due to the multiconfigurational character of this state, the theoretical difficulties encountered in previous studies. The computed oscillator strength is  $8.02 \times 10^{-2}$ , which corresponds to the observed value of  $8.8 \times 10^{-2}$ .

## C. Adiabatic excitation energies and interpretation of the photodetachment spectra

Adiabatic excitation energies,  $T_e$  and  $T_0$ , and the optimized geometry are summarized in Table IV. In the following, we show the adiabatic MRMP excitation energies with the state-specific CASSCF and those with the state-averaged CASSCF in parentheses. The calculated adiabatic excitation energies are  $^3A_2$ , 0.90 (0.96) eV,  $^1A_2$ , 1.15 (1.18) eV,  $^3B_2$ , 1.19 (1.20) eV,  $^3B_1$ , 1.18 (1.24) eV,  $^1B_1$ , 1.65 (1.67) eV, and  $^1B_2$ , 3.77 (3.79) eV, respectively. Again, there is little difference between the state-specific and state-averaged calculations. The ZPE corrections to the excitation energies are 0.01–0.02 eV in magnitude. The present theory predicts that the four lowest-lying excited states exist below 2 eV in energy above the ground state. The dissociation energy of the ground state is computed to be 0.834 eV ( $D_0=1.05$  eV;  $D_e=1.13$  eV) at the same level of theory. Thus, the present theory also predicts that none of the excited states lies below the ground state dissociation limit of  $O_3$ . The  $^1B_1$  and  $^1B_2$  states correlate with the dissociation limit,  $O(^1D)+O_2(^1\Delta_g)$  while the  $^3B_1$  correlates with  $O(^3P)+O_2(^1\Delta_g)$ . These states are predicted to lie below their dissociation limit of 4.08 and 2.11 eV, respectively. The present adiabatic excitation energies are very close to those with the original version of CASPT2 reported recently by Borowski *et al.*<sup>41</sup>

Previous calculations have predicted various orderings of the excited states, depending on the level of theory employed. While all of these states are fairly low-lying, the  $n \rightarrow \pi^*$   $^3A_2$  and  $\pi \rightarrow \pi^*$   $^3B_2$  states are usually found to be the lowest excited states. The MRD-CI, CASPT2( $g_2$ ), and MRMP predicted that the lowest excited state is the  $^3A_2$ . On the other hand, POL-CI and MCSCF-CI predicted the lowest excited states to be the  $^3B_2$  state. MRMP predicts that three states,  $^3B_2$ ,  $^3B_1$ , and  $^1A_2$ , following  $^3A_2$  appear at the range

TABLE III. Calculated and experimental oscillator strengths and vertical excitation energies in ozone.<sup>a</sup>

State	Method	Oscillator strength	Excitation energy (eV)
<sup>3</sup> A <sub>2</sub>	POL-CI <sup>b</sup>	0.0	2.09
	MCSCF-CI <sup>c</sup>	...	1.92
	MRD-CI <sup>d</sup>	0.0	1.44
	MCLR <sup>e</sup>	0.0	1.81
	FSMRCC <sup>f</sup>	0.0	1.95
	CASPT2 <sup>g</sup>	0.0	1.56
	CASPT2( <i>g</i> <sub>2</sub> ) <sup>g</sup>	0.0	1.77
	MRMP	0.0	1.65(1.57)
	Expt	...	...
	<sup>3</sup> B <sub>2</sub>	POL-CI	0.0
MCSCF-CI		...	1.14
MRD-CI		0.0	1.20
MCLR		0.0	1.14
FSMRCC		0.0	1.37
CASPT2		0.0	1.58
CASPT2( <i>g</i> <sub>2</sub> )		0.0	1.67
MRMP		0.0	1.71(1.56)
Expt		...	...
<sup>3</sup> B <sub>1</sub>		POL-CI	0.0
	MCSCF-CI	...	2.00
	MRD-CI	0.0	1.59
	MCLR	0.0	1.81
	FSMRCC	0.0	1.62
	CASPT2	0.0	1.45
	CASPT2( <i>g</i> <sub>2</sub> )	0.0	1.62
	MRMP	0.0	1.51(1.47)
	Expt	...	...
	<sup>1</sup> A <sub>2</sub>	POL-CI	0.0
MCSCF-CI		...	2.17
MRD-CI		0.0	1.72
MCLR		0.0	2.14
FSMRCC		0.0	2.17
CASPT2		0.0	1.77
CASPT2( <i>g</i> <sub>2</sub> )		0.0	2.03
MRMP		0.0	1.88(1.78)
Expt		...	1.6 <sup>h</sup>
<sup>1</sup> B <sub>1</sub>		POL-CI	4.0×10 <sup>-5</sup>
	MCSCF-CI	...	2.32
	MRD-CI	1.5×10 <sup>-5</sup>	1.95
	MCLR	7.3×10 <sup>-6</sup>	2.17
	FSMRCC	2.85×10 <sup>-5</sup>	2.13
	CASPT2	1.6×10 <sup>-5</sup>	1.87
	CASPT2( <i>g</i> <sub>2</sub> )	1.6×10 <sup>-5</sup>	2.11
	MRMP	2.20×10 <sup>-5</sup>	1.97(1.87)
	Expt	2.0×10 <sup>-5</sup>	2.1 <sup>h</sup>
	<sup>1</sup> B <sub>2</sub>	POL-CI	2.3×10 <sup>-1</sup>
MRD-CI		1.76×10 <sup>-1</sup>	4.97
MCLR		9.3×10 <sup>-2</sup>	5.10
FSMRCC		1.30×10 <sup>-1</sup>	5.52
CASPT2		8.9×10 <sup>-2</sup>	4.51
CASPT2( <i>g</i> <sub>2</sub> )		8.9×10 <sup>-2</sup>	4.69
MRMP		8.0×10 <sup>-2</sup>	4.81(4.62)
Expt		8.8×10 <sup>-2</sup>	4.86 <sup>h</sup>

<sup>a</sup>Values in parentheses are excitation energies calculated with MRMP based on the state-averaged CASSCF.

<sup>b</sup>Reference 38.

<sup>c</sup>Reference 12.

<sup>d</sup>Reference 9.

<sup>e</sup>Reference 40.

<sup>f</sup>Reference 39.

<sup>g</sup>Reference 41.

<sup>h</sup>Reference 3.

of 1.4–1.8 eV above the ground state. The CASPT2(*g*<sub>2</sub>) also placed <sup>3</sup>B<sub>2</sub> and <sup>3</sup>B<sub>1</sub> placed at the same position of 1.33 eV. We can see from Table I that <sup>3</sup>B<sub>2</sub> state is described well even by a single configuration but other excited states are of multiconfigurational character. Thus, the balanced description requires a careful treatment. Unless both the dynamical and nondynamical correlations are fully included, other excited states with multiconfigurational character will be placed at higher energies compared to the <sup>3</sup>B<sub>2</sub> state. This must be the reason why POL-CI and MCSCF-CI predicted the lowest excited states to be the <sup>3</sup>B<sub>2</sub> state.

Arnold *et al.*<sup>21</sup> studied the low-lying electronic states of ozone using photoelectron spectroscopy of O<sub>3</sub><sup>-</sup>. The spectra show photodetachment transitions from O<sub>3</sub><sup>-</sup> to the five lowest-lying electronic states in addition to the ground state of ozone. These correspond to excitation energies of 1.18, 1.30, 1.45, ~1.6, and 2.046 eV, respectively. The excited state spectra are dominated by bending vibrational progressions which, for some states, extend well above the dissociation asymptote without noticeable lifetime broadening effects. The geometric differences between the anion and neutral govern the Franck–Condon factors and thus the vibrational profile for each electronic state. Since the bond lengths of these excited states are approximately equal to that of the anion except <sup>1</sup>B<sub>2</sub>, very little excitation of the symmetric stretch is expected for any of the excited states. For <sup>1</sup>B<sub>2</sub> state, significant difference is found in the bond length compared to that of the anion. But this state is not measured in the photodetachment experiment of Arnold *et al.* Anderson *et al.*<sup>3,4</sup> also obtained independent evidence that excited states may exist at excitation energies of 1.1833, 1.29, and 1.45 eV using absorption and isotropic substitution techniques. However, no evidence for an excited state with ~1.6 eV has been found in any absorption spectra as of yet.

As to the optimized geometries for excited states, reasonable agreement is found with the previous theoretical values. A slight disagreement is found for the bond length of the <sup>1</sup>B<sub>2</sub> state. The <sup>1</sup>B<sub>2</sub> potential energy surface near the minimum is very flat but our bond length gives 1.470 Å which is longer by about 0.1 Å than the previous results. However, excellent agreement is found for bond angles. Based on our computed results shown in Fig. 2, one can expect significant bending mode excitation upon photodetachment of the ozonide anion for both the <sup>3</sup>A<sub>2</sub> and <sup>1</sup>A<sub>2</sub> states, medium length progressions for <sup>3</sup>B<sub>2</sub> and <sup>3</sup>B<sub>1</sub> states and very little excitation for <sup>1</sup>B<sub>1</sub> and <sup>1</sup>B<sub>2</sub> states.

Arnold *et al.*<sup>21</sup> assigned that the lowest excited states are the <sup>3</sup>A<sub>2</sub> state with a long vibrational progression. The corresponding excitation energies are determined to be 1.18 eV. Our excitation energy is 0.90 eV for the <sup>3</sup>A<sub>2</sub> state. A large difference of the bond angle between the ozonide anion ( $\theta_e = 115.5^\circ$ ) and the <sup>3</sup>A<sub>2</sub> state ( $\theta_e = 99.2^\circ$ ) suggests the significant bending mode excitation upon photodetachment of the ozonide anion. MRMP also confirms their assignment that the lowest excited state is the <sup>3</sup>A<sub>2</sub> state. The Wulf band was found to have a long progression in the bend superimposed on a shorter progression in the stretch.<sup>3,4</sup> This is consistent with the calculated geometry difference between the

TABLE IV. Calculated and experimental geometries and adiabatic excitation energies in ozone.<sup>a</sup>

State	Method	Bond length (angstrom)	Bond angle (degree)	Excitation energy (eV)	
				$T_e$	$T_0$
$^1A_1$	POL-CI <sup>b</sup>	1.299	116.0	0.00	0.00
	MCSCF-CI <sup>c</sup>	1.277	116.1	0.00	0.00
	MRD-CI <sup>d</sup>	1.29	116.0	0.00	0.00
	CASPT2 <sup>e</sup>	1.287	116.8	0.00	0.00
	CASPT2( $g_2$ ) <sup>e</sup>	1.284	116.9	0.00	0.00
	MRMP	1.291	116.6	0.00	0.00
	Expt	1.2717	116.7	0.00	0.00
$^3A_2$	POL-CI	1.366	99.7	1.35	1.33
	MCSCF-CI	1.348	101.5	1.34	1.33
	MRD-CI	1.36	103.6	0.86	0.86
	CASPT2	1.350	98.6	0.96	0.95
	CASPT2( $g_2$ )	1.344	97.8	1.16	1.15
	MRMP	1.369	99.2	0.90 (0.96)	0.92
	Expt	...	...	...	1.18, <sup>f</sup> 1.24 <sup>g</sup>
$^3B_2$	POL-CI	1.382	107.9	0.92	0.91
	MCSCF-CI	1.360	108.3	1.09	1.09
	MRD-CI	1.34	108.5	1.10	1.10
	CASPT2	1.365	108.9	1.23	1.22
	CASPT2( $g_2$ )	1.363	108.9	1.34	1.33
	MRMP	1.379	108.3	1.19 (1.20)	1.18
	Expt	...	...	...	1.30 <sup>f</sup>
$^3B_1$	POL-CI	1.347	123.8	1.74	1.71
	MCSCF-CI	1.343	121.3	1.34	1.31
	MRD-CI	1.36	123.5	1.27	1.27
	CASPT2	1.319	128.1	1.22	1.20
	CASPT2( $g_2$ )	1.310	129.8	1.35	1.33
	MRMP	1.348	123.7	1.18 (1.24)	1.16
	Expt	...	...	...	1.45 <sup>f</sup>
$^1A_2$	POL-CI	1.374	100.7	1.66	1.64
	MCSCF-CI	1.351	101.5	1.57	1.56
	MRD-CI	1.34	100.0	1.44	1.44
	CASPT2	1.355	99.3	1.20	1.19
	CASPT2( $g_2$ )	1.348	98.5	1.45	1.44
	MRMP	1.374	99.7	1.15 (1.18)	1.14
	Expt	...	...	...	~1.6 <sup>f</sup>
$^1B_1$	POL-CI	1.370	117.7	2.06	2.03
	MCSCF-CI	1.362	116.2	2.01	1.98
	MRD-CI	1.35	117.2	1.82	1.81
	CASPT2	1.340	122.6	1.67	1.65
	CASPT2( $g_2$ )	1.325	125.6	1.90	1.88
	MRMP	1.376	117.4	1.65 (1.67)	1.64
	Expt	...	...	...	2.05 <sup>g</sup>
$^1B_2$	POL-CI	1.405	108.4	5.54	...
	MRD-CI	1.38	110.1	4.34	4.34
	CASPT2	1.427	110.7	3.87	3.84
	CASPT2( $g_2$ )	1.416	109.8	4.08	4.05
	MRMP	1.470	111.6	3.77 (3.79)	3.76
	Expt	...	...	...	3.41 <sup>g</sup>

<sup>a</sup>Values in parentheses are excitation energies calculated with MRMP based on the state-averaged CASSCF. Zero-point energy corrections in  $T_0$  were estimated with  $\nu_1$  and  $\nu_2$ .

<sup>b</sup>Reference 38.

<sup>c</sup>Reference 12.

<sup>d</sup>Reference 9.

<sup>e</sup>Reference 41.

<sup>f</sup>Reference 21.

<sup>g</sup>Reference 3.

ground state and the  $^3A_2$  state. The Wulf band structure is most likely due to the  $^3A_2$  state.

The two peaks following  $^3A_2$  appear at 1.30 and 1.45 eV, respectively, with a short or a medium length vibrational progression. Arnold *et al.* assigned the first peak due to the  $^3B_2$  state and the second peak due to the  $^3B_1$  based on the

previous theoretical results that the  $^3B_2$  is much lower in energy than the  $^3B_1$ . However, MRMP predicted that both  $^3B_2$  and  $^3B_1$  states appear at 1.19 and 1.18 eV, respectively. The geometry change as shown in Fig. 2 also suggests that a medium length  $\nu_2$  progression is expected on the photodetachment pattern both for the  $^3B_1$  ( $r_e=1.348$  Å,  $\theta_e=123.7^\circ$ )

and  ${}^3B_2$  ( $r_e = 1.379$  Å,  $\theta_e = 108.3^\circ$ ). Thus, the simple considerations of geometry and energy are insufficient to determine a specific assignment of these states. The most recent CASPT2 also showed the similar trend to the present results.

The  ${}^3B_2$  state is dominated by a  $\pi-\pi^*$  single excitation while the  ${}^3B_1$  state is a singly excited state from the in-plane  $6a_1$  lone-pair orbitals to  $2b_1\pi^*$  orbital, perpendicular to the molecular plane. The difference of the electronic configurations may reflect in the dependence of the features in the photoelectron spectrum on the laser polarization direction.

Vertically  ${}^3B_1$  lies slightly below  ${}^3A_2$ . Adiabatically, however,  ${}^3A_2$  moves well below  ${}^3B_1$ . As shown in Fig. 2,  ${}^3A_2$  and  ${}^3B_1$  states are close in energy and have a seam. The existence of such an intersection in  $C_{2v}$  constrained symmetry has been studied previously.<sup>7,8</sup> The seam is crossing in the Franck–Condon region and also near the minimum region of  ${}^3A_2$  which becomes a conical intersection in  $C_s$  symmetry, where these states become the lowest two  ${}^3A''$  states. The lower state is dissociative; it has a saddle point (where it is  ${}^3A_2$ ) and displacement from the saddle point leads to the ground electronic state  $O_2({}^3\Sigma_g^-) + O({}^3P)$  products. The upper state (the cone state) is bound ( ${}^3B_1$  at its minimum) and can support vibrational levels. It correlates with electronically excited  $O_2({}^1\Delta_g) + O({}^3P)$  products. Every vibrational state of  ${}^3B_1$  manifold will extend with appreciable amplitude across this intersection. This feature of the surface will have a profound effect on the photoabsorption and photodissociation dynamics. This may provide information to determine the specific assignment.

The photodetachment spectra show that the next peak has a long  $\nu_2$  progression, corresponding to the transition energy of  $\sim 1.6$  eV. Arnold *et al.*<sup>21</sup> assigned tentatively that the peak with a long progression is due to the  ${}^1A_2$  state. The simple consideration of geometry suggests that a long  $\nu_2$  progression is expected for the  ${}^1A_2$  state. The  ${}^1A_2$  state has a large enough difference in bond angle from the ozonide anion to be consistent with the observed long bending progression. MRMP also confirms that the peak is due to the  ${}^1A_2$  state. However, the present theory predicts the  ${}^1A_2$  state lies at 1.15 eV above the ground state. There is some discrepancy between theory and experiment for the position of the  ${}^1A_2$  state. On the other hand, Anderson *et al.*<sup>3,4</sup> has determined the adiabatic excitation energy of the  ${}^1A_2$  state as 1.24 eV, studying the isotopic shifts between the absorption spectra of  ${}^{16}O_3$  and  ${}^{18}O_3$ . However, the absorption was reassigned to the  ${}^3A_2$  by an analysis of the rotational structure of the spectrum.<sup>5</sup>

The optimized geometry of singlet and triplet  $A_2$  states is very similar and both states are dominated by the single excitation  $4b_2 \rightarrow 2b_1$ ; the  $4b_2$  is the in-plane orbital while the  $2b_1$  is  $\pi^*$  orbital. Hence we expect that the energy splitting between singlet and triplet is rather small. The computed energy splitting is 0.25 eV while the splitting estimated by Arnold *et al.* is 0.42 eV. At present we cannot explain the discrepancy between theory and experiment on the position of the  ${}^1A_2$  state.

The next excited state is the  ${}^1B_1$  state, which is computed to appear at 1.65 eV. The Chappuis band absorption were tentatively assigned to the transition to the  ${}^1B_1$  state

( $T_e = 2.046$  eV). The  ${}^1B_1$  state has its minimum at  $r_e = 1.376$  Å and  $\theta_e = 117.4^\circ$ . The  ${}^1B_1$  equilibrium geometry is very close to that of ozonide anion. This suggests that the photo-detachment pattern from the anion is primarily governed by the Franck–Condon factors. On the other hand, the absorption spectra of Chappuis band have a long progression in the symmetric stretch and a short progression in the bend.<sup>3,4</sup> We can see from Table IV that there is a significant difference in the bond length between the ground and the  ${}^1B_1$  state while bond angles are very close. The present results also support the assignment that the Chappuis band originates from the  ${}^1B_1$  state.

The singlet  $A_2$  and  $B_1$  states also have a seam crossing in the Franck–Condon region as shown in Fig. 2. The lower state leads to the ground electronic state of  $O_2({}^3\Sigma_g^-) + O({}^3P)$  and the upper state will lead to the excited  $O_2({}^1\Delta_g) + O({}^1D)$  state.

The  $\pi-\pi^*$   ${}^1B_2$  state is the upper state of the intense Hartley bands. The minimum energy of the  ${}^1B_2$  state is found at  $r_e = 1.470$  Å and  $\theta_e = 111.6^\circ$ . The present calculations reproduced longer bond length by 0.06–0.09 Å compared to the previous calculations. The contour lines (Fig. 2) characterize the state as possessing a very wide potential well. The MRMP predicts the  ${}^1B_2$  state lies at 3.77 eV above the ground state. The agreement between theory (3.77 eV) and experiment (3.41 eV) is satisfactory. The  ${}^1B_2$  state is of ionic character and previous theoretical calculations place this transition at higher energies.

#### IV. CONCLUSIONS

To conclude, the geometry and relative energy of the seven low-lying electronic states of ozone and the ground state of ozonide anion have been determined in  $C_{2v}$  symmetry by CASSCF and multireference Møller–Plesset perturbation methods. The results are compared with the photodetachment spectra of  $O_3^-$  observed recently by Arnold *et al.* The theoretical electron affinity of ozone is 1.965 eV, which is 0.14 eV below the experimental result of 2.103 eV. The calculated adiabatic excitation energies,  $T_e$  (assignment of Arnold *et al.* in parentheses) of ozone are  ${}^3A_2$  0.90 eV (1.18 eV),  ${}^3B_2$ , 1.19 eV (1.30 eV),  ${}^3B_1$ , 1.18 eV (1.45 eV),  ${}^1A_2$ , 1.15 eV ( $\sim 1.6$  eV),  ${}^1B_1$ , 1.65 eV (2.05 eV), and  ${}^1B_2$ , 3.77 eV (3.41 eV), respectively. Overall the present theory supports the assignment of Arnold *et al.* However, the simple considerations of geometry and energy are insufficient to determine a specific assignment of the  ${}^3B_2$  and  ${}^3B_1$  states. The dissociation energy of the ground state of ozone is computed to be 0.834 eV at the present level of theory. The present theory also predicts that none of the excited states lies below the ground state dissociation limit of  $O_3$ .

For the complete assignment of the spectra and the understanding of the excited state dissociation dynamics, we need further calculations including the quantitative potential surface not just the restricted (two-dimensional)  $C_{2v}$  space but the full (three-dimensional)  $C_s$  space and the time-dependent wave packet dynamics. The study in this line is now going on and will be published in the forthcoming publications.

## ACKNOWLEDGMENTS

The present research is supported in part by the Grant-in-Aid for Scientific Research on Priority Area "Theory of Chemical Reactions" from the Ministry of Education, Science, and Culture. The computations were carried out on the IBM RS6000-590 workstations at IMS. The CASSCF reference wave functions were obtained by the MOLPRO program.<sup>42</sup> The perturbation calculations were performed with the MR2D program.<sup>43</sup>

- <sup>1</sup>M. J. Chappuis, C. R. Acad. Sci. (Paris) **91**, 1985 (1880).
- <sup>2</sup>O. R. Wulf, Proc. Natl. Acad. Sci. **16**, 507 (1930).
- <sup>3</sup>S. M. Anderson, J. Morton, and K. Mauersberger, J. Chem. Phys. **93**, 3826 (1990).
- <sup>4</sup>S. M. Anderson, J. Maeder, and K. Mauersberger, J. Chem. Phys. **94**, 6351 (1991).
- <sup>5</sup>S. M. Anderson, P. Hupalo, and K. Mauersberger, J. Chem. Phys. **99**, 737 (1993).
- <sup>6</sup>V. Vaida, D. J. Donaldson, S. J. Strickler, S. L. Stephens, and J. W. Birks, J. Phys. Chem. **93**, 506 (1989).
- <sup>7</sup>M. Braunstein, P. J. Hay, R. L. Martin, and R. T Pack, J. Chem. Phys. **95**, 8239 (1991).
- <sup>8</sup>M. Braunstein and R. T Pack, J. Chem. Phys. **96**, 6378 (1992).
- <sup>9</sup>K. H. Thunemann, S. D. Peyerimhoff, and R. J. Buenker, J. Mol. Spectrosc. **70**, 432 (1978).
- <sup>10</sup>A. Banichevich, S. D. Peyerimhoff, and F. Grein, Chem. Phys. Lett. **173**, 1 (1990).
- <sup>11</sup>A. Banichevich, S. D. Peyerimhoff, J. A. Beswick, and O. Atabek, J. Chem. Phys. **96**, 6580 (1992).
- <sup>12</sup>A. Banichevich and S. D. Peyerimhoff, Chem. Phys. **174**, 93 (1993).
- <sup>13</sup>J. R. Locker, J. A. Jones, and E. J. Bair, J. Photochem. **36**, 235 (1987).
- <sup>14</sup>T. Kleindienst, J. R. Locker, and E. J. Bair, J. Photochem. **12**, 67 (1980).
- <sup>15</sup>C. W. von Rosenberg and D. W. Trainor, J. Chem. Phys. **63**, 5348 (1975).
- <sup>16</sup>J. Shi and J. R. Barker, J. Phys. Chem. **94**, 8390 (1990).
- <sup>17</sup>W. D. McGrath, J. M. Maguire, A. Thompson, and J. Trocha-Grimshaw, Chem. Phys. Lett. **102**, 59 (1983).
- <sup>18</sup>N. Swanson and R. J. Celotta, Phys. Rev. Lett. **35**, 783 (1975).
- <sup>19</sup>K. A. Peterson, R. C. Mayrhofer, and R. C. Woods, J. Chem. Phys. **93**, 5020 (1990).
- <sup>20</sup>P. G. Burton and M. D. Harvey, Nature **266**, 826 (1977).
- <sup>21</sup>D. W. Arnold, C. Xu, E. H. Kim, and D. M. Neumark, J. Chem. Phys. **101**, 912 (1994).
- <sup>22</sup>P. C. Cosby, J. T. Moseley, J. R. Peterson, and J. H. Ling, J. Chem. Phys. **69**, 2771 (1978); J. F. Hiller and M. L. Vestal, *ibid.* **74**, 6096 (1981).
- <sup>23</sup>L. J. Wang, S. B. Woo, and E. M. Helmy, Phys. Rev. A **35**, 759 (1987).
- <sup>24</sup>S. E. Novick, P. C. Engelking, P. L. Jones, J. H. Futrell, and W. C. Lineberger, J. Chem. Phys. **70**, 2652 (1979).
- <sup>25</sup>K. Hirao, Chem. Phys. Lett. **190**, 374 (1992).
- <sup>26</sup>K. Hirao, Chem. Phys. Lett. **196**, 397 (1992).
- <sup>27</sup>K. Hirao, Chem. Phys. Lett. **201**, 59 (1993).
- <sup>28</sup>K. Hirao, Int. J. Quantum Chem. **S26**, 517 (1992).
- <sup>29</sup>K. Hirao, H. Nakano, and T. Hashimoto, Chem. Phys. Lett. **235**, 430 (1995).
- <sup>30</sup>D. H. Dunning, J. Chem. Phys. **90**, 1007 (1989).
- <sup>31</sup>P. E. Siegbahn, A. Heiberg, B. O. Roos, and B. Levy, Phys. Scr. **21**, 323 (1980).
- <sup>32</sup>B. O. Roos, P. R. Taylor, and P. E. Siegbahn, Chem. Phys. **48**, 157 (1980).
- <sup>33</sup>B. O. Roos, Int. J. Quantum Chem. **S14**, 175 (1980).
- <sup>34</sup>K. Ohta, H. Nakatsuji, K. Hirao, and T. Yonezawa, J. Chem. Phys. **73**, 1770 (1980).
- <sup>35</sup>W. Koch, G. Frenking, G. Steffen, D. Reinen, M. Jansen, and W. Assenmacher, J. Chem. Phys. **99**, 1271 (1993).
- <sup>36</sup>R. Gonzalez-Luque, M. Merchan, P. Borowski, and B. O. Roos, Theor. Chim. Acta **86**, 467 (1993).
- <sup>37</sup>P. J. Hay, T. H. Dunning, and W. A. Goddard, Chem. Phys. Lett. **23**, 457 (1973).
- <sup>38</sup>P. J. Hay and T. H. Dunning, J. Chem. Phys. **67**, 2290 (1977).
- <sup>39</sup>M. Barysz, M. Rittby, and R. J. Bartlett, Chem. Phys. Lett. **193**, 373 (1992).
- <sup>40</sup>D. Nordfors, H. Ågren, and H. J. A. Jensen, Int. J. Quantum Chem. **40**, 475 (1990).
- <sup>41</sup>P. Borowski, M. Fülscher, P.-A. Malmqvist, and B. O. Roos, Chem. Phys. Lett. **237**, 195 (1995).
- <sup>42</sup>MOLPRO is a package of *ab initio* programs written by H.-J. Werner and P. J. Knowles: H.-J. Werner and P. J. Knowles, J. Chem. Phys. **73**, 2342 (1980); P. J. Knowles and H.-J. Werner, Chem. Phys. Lett. **115**, 259 (1985).
- <sup>43</sup>H. Nakano, J. Chem. Phys. **99**, 7983 (1993); MR2D, Version 2, H. Nakano, University of Tokyo.